SUPPLEMENTARY DATA
Bois, B., Nicolas, S., Roig Puscama, F., Giraudo, J., Rega, M., Gavrilescu, C., … Ouvrié, M. Methodological considerations on local temperature zoning: where to install sensors, how many sensors and what interpolation method could be used? A case study in Morey-Saint-Denis and Chambolle Musigny (Bourgogne, France): Original research article Special Issue TERCLIM2026. *OENO One, 60*(3).
https://doi.org/10.20870/oeno-one.2026.60.3.9882

SUPPLEMENTARY DATA

Table S1. List of terrain descriptors used for spatial interpolation of data.

	Prefix/Acronym	Relief Descriptor	Detail	Référence
1	RGE5mLiss	Elevation	Elevation derived from the 5 m resolution DEM (RGE Alti ®; IGN)	https://geoservices.ign.fr/rgealti
2	RelSlopePosition	Relative slope position index	Relative elevation difference compared to thalwegs and ridges	(Bock *et al*., 2007)
3	AspCosinusNS	Cosine of slope aspect	Index of slope orientation towards the north or south	
4	AspSinusEW	Sine of slope aspect	Index of slope orientation towards the east or west	
5	SLOPE	Slope	Average slope of a pixel	(Zevenbergen & Thorne, 1987)
6	PISR	Potential direct irradiation at equinox	Indicates the cumulative daily direct solar radiation [kWh/m²] under clear sky conditions at a latitude of 47.2 degrees, calculated hourly from March 20th in the northern hemisphere	(Böhner & Antonić, 2009)
7	TWI	Topographic Wetness Index	Topographic Wetness Index (TWI) or SAGA Wetness Index (SWI) are indicators of water or cold air accumulation in case of radiative frost, based on the calculation of the upstream catchment area relative to the slope of the pixel of interest	(Bock *et al*., 2007; Böhner *et al*., 2006; Kopecký *et al*., 2021)
8	SWI	Topographic Wetness Index	See TWI	
9	Log_ModCathArea	Logarithm of the modified upstream catchment area	Calculation of the upstream catchment area, *i.e.*, the sum of the cells (pixels) from which water is collected in each pixel	(Böhner *et al*., 2002, 2006)
10	PosOpeness_100	Landscape openness	Average of the angles to the lowest point in 8 directions around the point of interest (within a radius of 100 meters). Indicates if the point is exposed.	(Prima *et al.*, 2006; Yokoyama *et al*., 2002)
11	PosOpeness_10000		Identical to PosOpen_100, but for a radius of 10 km.	
12	NegOpeness_100	Landscape enclosure	Average of the angles to the highest point in 8 directions around the point of interest (within a radius of 100 meters). Indicates if the point is enclosed.	(Prima *et al*., 2006; Yokoyama *et al*., 2002)

13	NegOpeness_10000		Identical to NegOpen_100, but for a radius of 10 km.	(Prima *et al.*, 2006; Yokoyama *et al*., 2002)
14	ValleyDepth	Valley depth	Difference between the elevation of a point and the ceiling defined by the surrounding ridges	(Bock *et al*., 2007)
15	WindEff_22.5	Wind exposure	Index of the degree of exposure to north-northeast wind (22.5°).	(Böhner & Antonić, 2009; Gerlitz *et al.*, 2015)
16	WindEff_90	Wind exposure	Index of the degree of exposure to east wind (90°).	(Böhner & Antonić, 2009; Gerlitz *et al*., 2015)
17	WindEff_202.5	Wind exposure	Index of the degree of exposure to west-southwest wind (202.5°).	(Böhner & Antonić, 2009; Gerlitz *et al*., 2015)
18	WindEff_270	Wind exposure	Index of the degree of exposure to west wind (270°).	(Böhner & Antonić, 2009; Gerlitz *et al*., 2015)
19	WindEff_315	Wind exposure	Index of the degree of exposure to west wind (315°).	(Böhner & Antonić, 2009; Gerlitz *et al*., 2015)

19 descriptors are derived from the relief analysis using SAGA GIS modules. They are calculated on the raw DTM, as well as a smoothed version of the DTM over a 100 m window. This gives a total of 19 x 2 = 38 descriptors derived from the relief analysis.

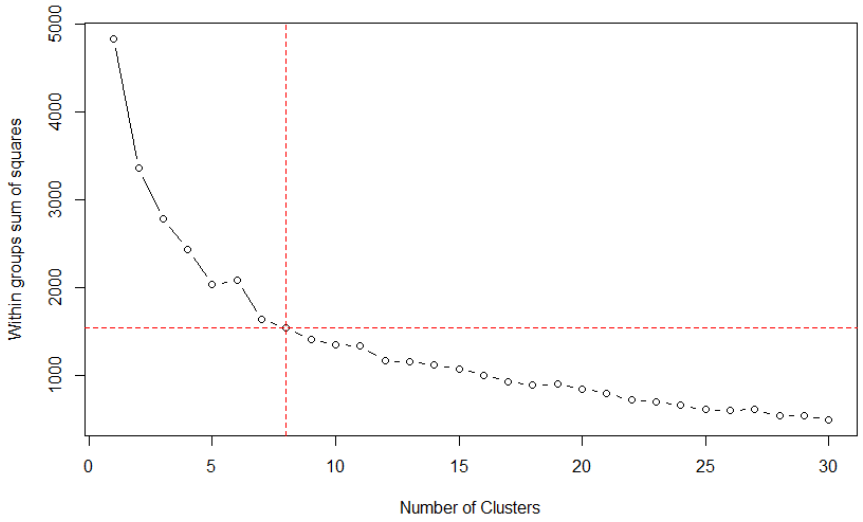


Figure S1. Within groups sum of squares (WSS) of each cluster according to the number of clusters.

The red dashed lines indicate the corresponding WSS to 8 clusters, considered as a good balance between cluster number and intra-group dispersion. See Makles (2012) for further information concerning the WSS approach.

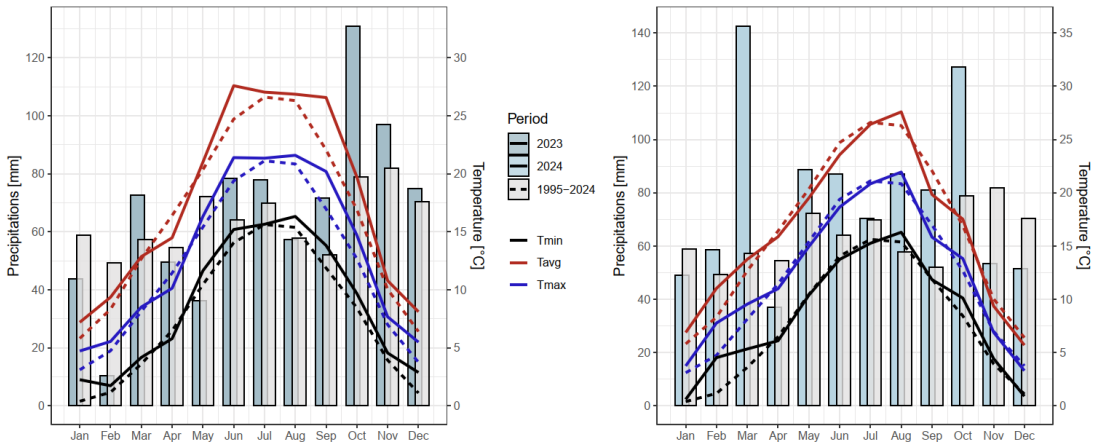


Figure S2. Monthly precipitation and minimum, average and maximum temperature of vintages 2023 (a) and 2024 (b), compared to 1995–2025 averages. Climate data from Dijon-Longvic weather station (Longitude = 5.088, Latitude = 47.268, Elevation = 219 asl from Météo-France).

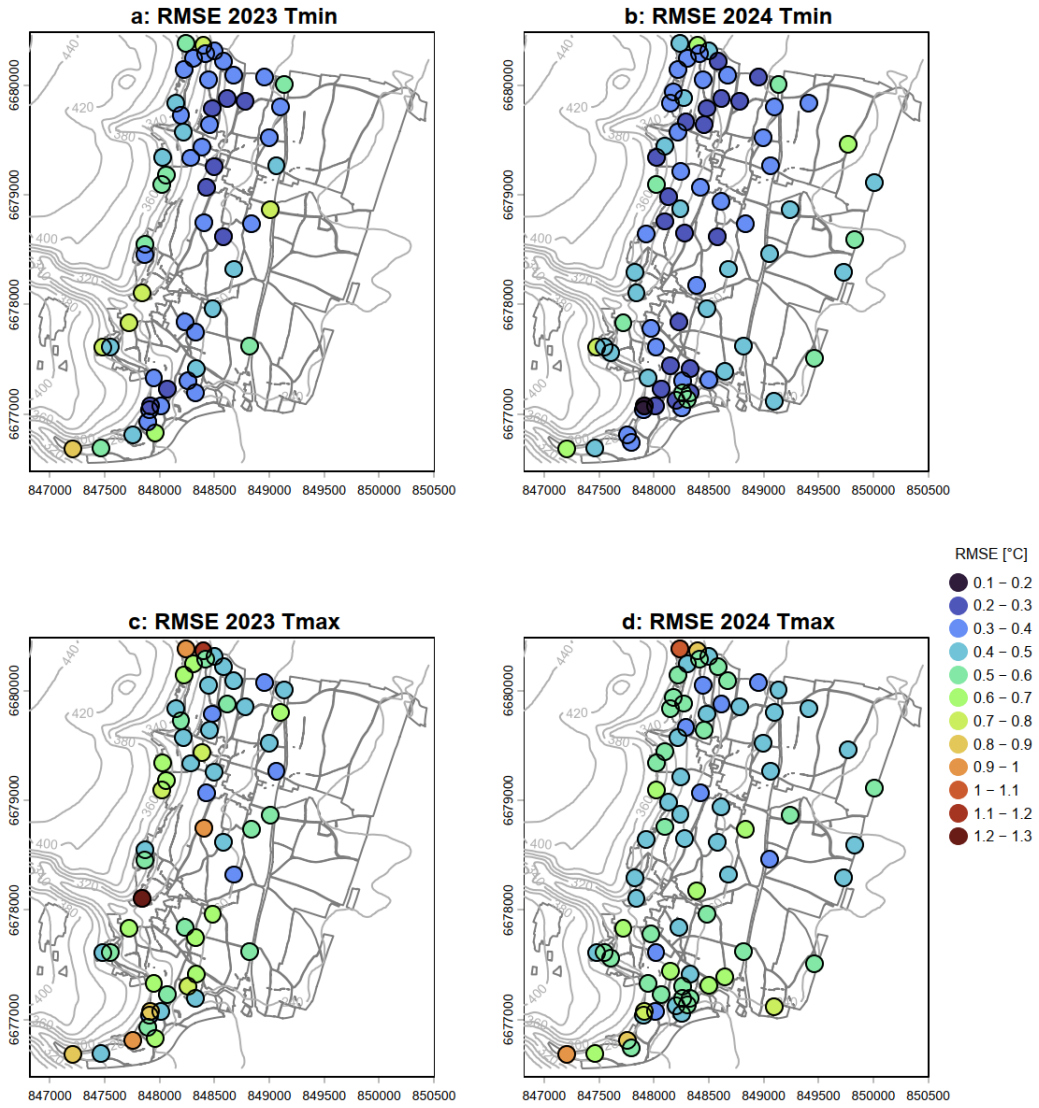


Figure S3. Spatial distribution of the root mean squared errors (RMSE) in the spatial interpolation of daily minimum (a and b) and maximum (c and d) temperatures using regression kriging in 2023 (a, c) and 2024 (b and d). The RMSE is calculated from the results of leave-one-out cross-validation. Note that only sensors having 2 % or less missing daily values (in comparison with the sensor that has the highest number of non-missing values) are plotted.

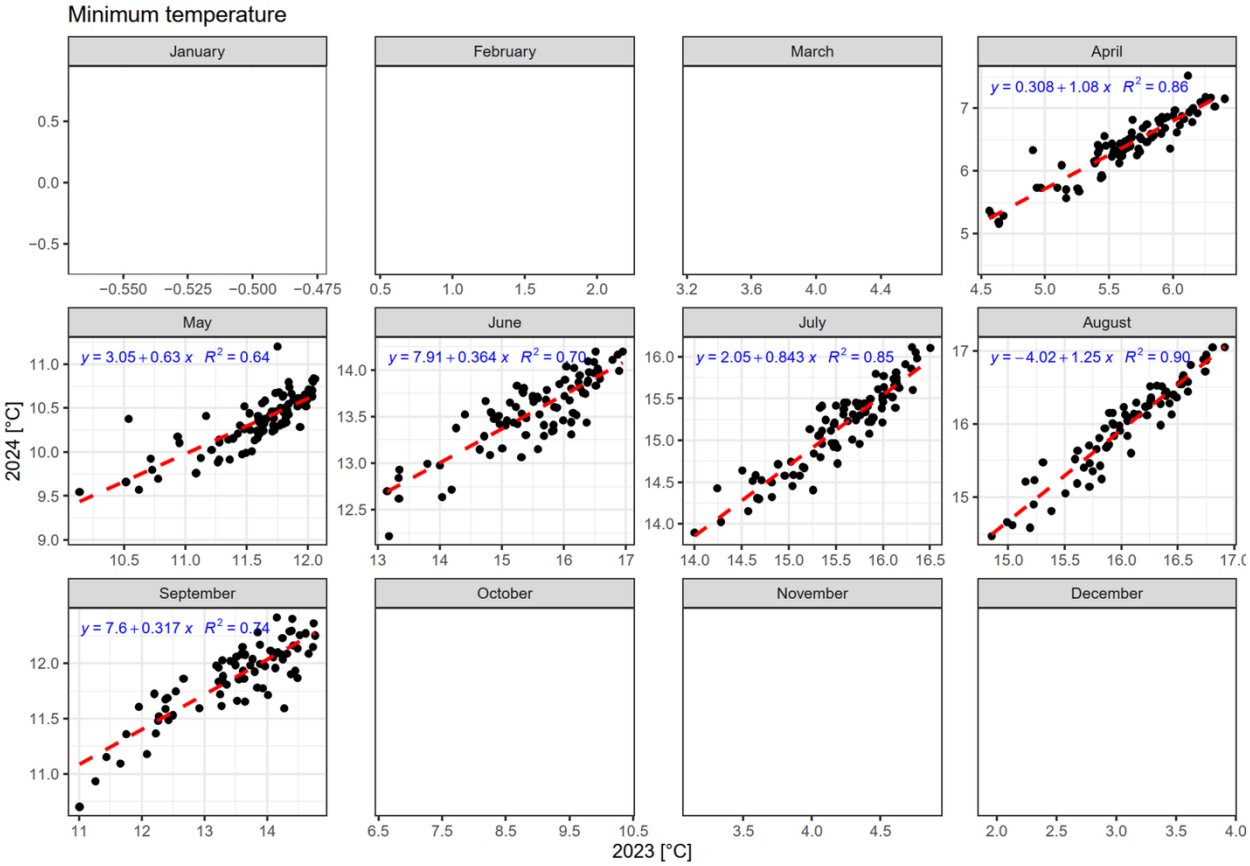


Figure S4. Comparison of 2023 and 2024 minimum temperature spatial distribution. Each dot corresponds to the monthly average of daily minimum temperatures at one sensor (*i.e.*, location).

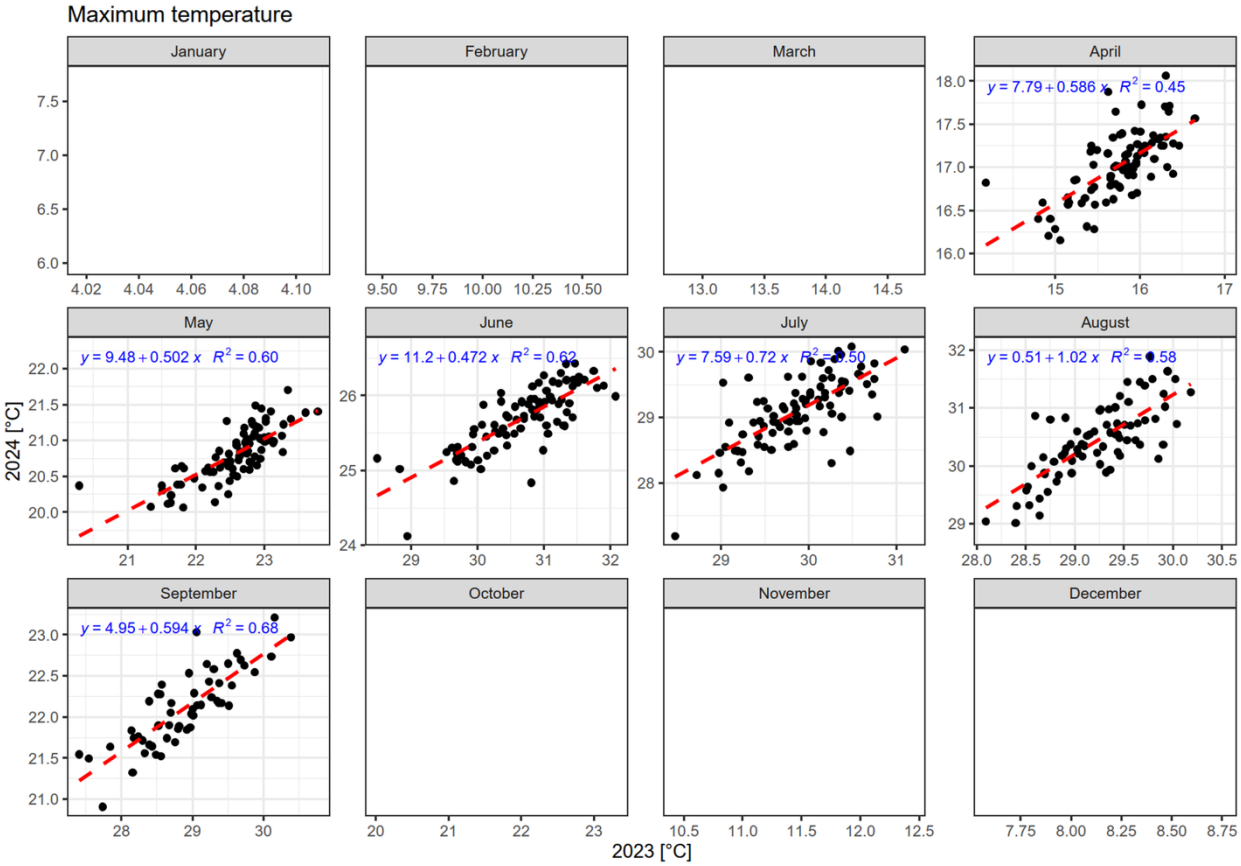


Figure S5. Comparison of 2023 and 2024 maximum temperature spatial distribution. Each dot corresponds to the monthly average of daily maximum temperatures at one sensor (*i.e.*, location).

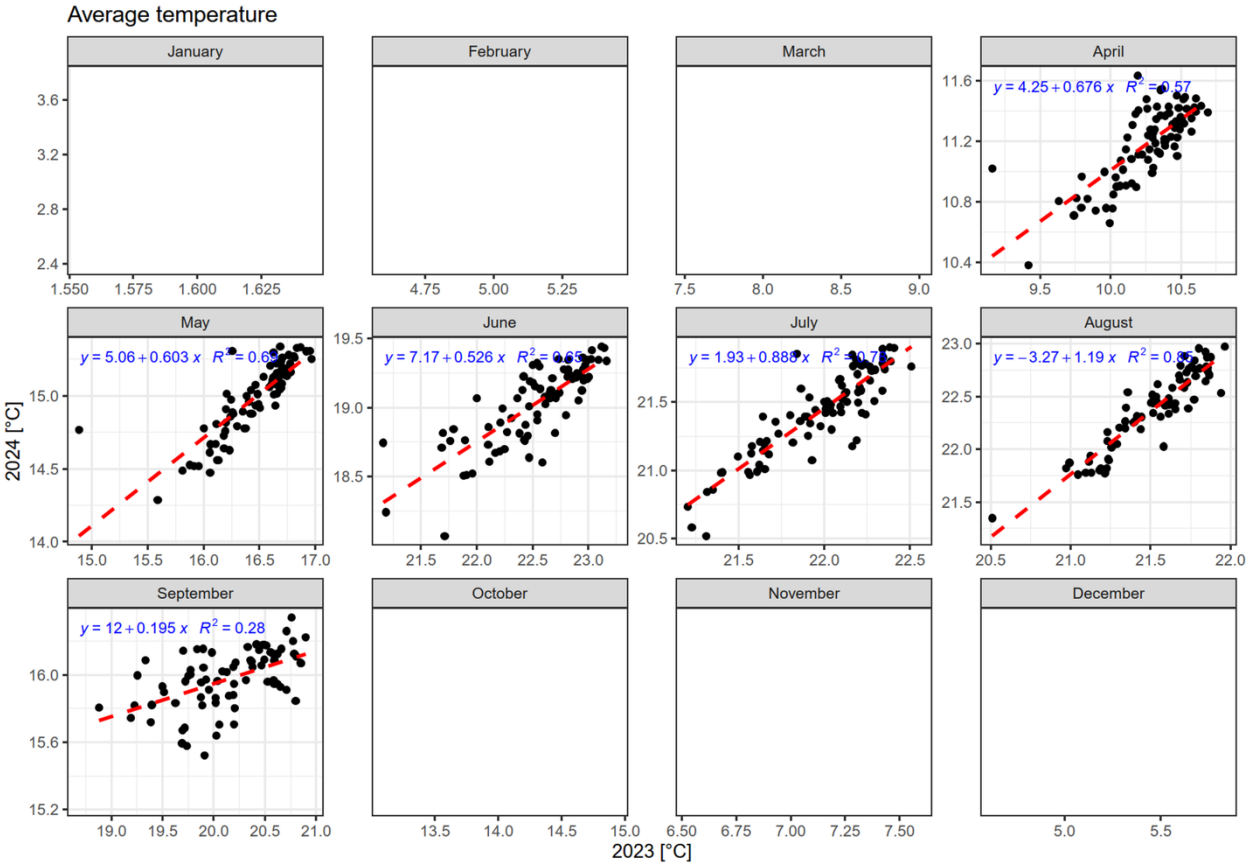


Figure S6. Comparison of 2023 and 2024 average temperature spatial distribution. Each dot corresponds to the monthly average of daily average temperatures at one sensor (*i.e.*, location).

References

Bock, M., Böhner, J., Conrad, O., Köthe, R., & Ringeler, A. (2007). XV. Methods for creating Functional Soil Databases and applying Digital Soil Mapping with SAGA GIS. In T. Hengl, P. Panagos, A. Jones, & G. Tóth, *Status and prospect of soil information in south-eastern Europe: Soil databases, projects and applications* (pp. 149–163). Office for Official Publications of the European Communities.

Böhner, J., & Antonić, O. (2009). Chapter 8 Land-Surface Parameters Specific to Topo-Climatology. In T. Hengl & H. I. Reuter (Eds), *Geomorphometry: Concepts, Software, Applications* (Vol. 33, pp. 195–226). Elsevier. http://www.sciencedirect.com/science/article/pii/S0166248108000081

Böhner, J., Koethe, R., Conrad, O., Gross, J., Ringeler, A., & Selige, T. (2002). Soil regionalisation by means of terrain analysis and process parameterisation. In E. Micheli, F. Nachtergaele, & L. Montanarella (Eds), *Research Report No. 7* (pp. 213–222). European Soil Bureau.

Böhner, J., McCloy, K. R., & Strobl, J. (Eds). (2006). SAGA - Analysis and Modelling Applications. *Göttinger Geographische Abhandlungen*, *115*, 1–116.

Gerlitz, L., Conrad, O., & Böhner, J. (2015). Large-scale atmospheric forcing and topographic modification of precipitation rates over High Asia – a neural-network-based approach. *Earth System Dynamics*, *6*(1), 61–81. https://doi.org/10.5194/esd-6-61-2015

Kopecký, M., Macek, M., & Wild, J. (2021). Topographic Wetness Index calculation guidelines based on measured soil moisture and plant species composition. *Science of The Total Environment*, *757*, 143785. https://doi.org/10.1016/j.scitotenv.2020.143785

Makles, A. (2012). Stata Tip 110: How to Get the Optimal K-Means Cluster Solution. *The Stata Journal: Promoting Communications on Statistics and Stata*, *12*(2), 347–351. https://doi.org/10.1177/1536867X1201200213

Prima, O. D. A., Echigo, A., Yokoyama, R., & Yoshida, T. (2006). Supervised landform classification of Northeast Honshu from DEM-derived thematic maps. *Geomorphology*, *78*(3), 373–386. https://doi.org/10.1016/j.geomorph.2006.02.005

Yokoyama, R., Shlrasawa, M., & Pike, R. J. (2002). Visualizing Topography by Openness: A New Application of Image processing to Digital Elevation Models. *Photogrammetric Engineering & Remote Sensing*, *68*(3), 257–265.

Zevenbergen, L. W., & Thorne, C. R. (1987). Quantitative analysis of land surface topography. *Earth Surface Processes and Landforms*, *12*(1), 47–56. https://doi.org/10.1002/esp.3290120107